NASA/ TM–20260001875

Modeling Study of Hatch Spacing's Effect on Grain Morphology in Repairing Damaged Metal Parts with Welding and Hatch Spacing's Potential Use in Lunar Exploration

Fredrick N. Michael
Marshall Space Flight Center, Huntsville, Alabama

Wei Li
The University of Texas at Dallas, Richardson, Texas

May 2026

NASA STI Program Report Series

The NASA STI Program collects, organizes, provides for archiving, and disseminates NASA's STI. The NASA STI Program provides access to the NTRS Registered and its public interface, the NASA Technical Reports Server, thus providing one of the largest collections of aeronautical and space science STI in the world. Results are published in both non-NASA channels and by NASA in the NASA STI Report Series, which includes the following report types:

- TECHNICAL PUBLICATION. Reports of completed research or a major significant phase of research that present the results of NASA Programs and include extensive data or theoretical analysis. Includes compilations of significant scientific and technical data and information deemed to be of continuing reference value. NASA counterpart of peer-reviewed formal professional papers but has less stringent limitations on manuscript length and extent of graphic presentations.

- TECHNICAL MEMORANDUM. Scientific and technical findings that are preliminary or of specialized interest, e.g., quick release reports, working papers, and bibliographies that contain minimal annotation. Does not contain extensive analysis.

- CONTRACTOR REPORT. Scientific and technical findings by NASA-sponsored contractors and grantees.

- CONFERENCE PUBLICATION. Collected papers from scientific and technical conferences, symposia, seminars, or other meetings sponsored or co-sponsored by NASA.

- SPECIAL PUBLICATION. Scientific, technical, or historical information from NASA programs, projects, and missions, often concerned with subjects having substantial public interest.

- TECHNICAL TRANSLATION. English-language translations of foreign scientific and technical material pertinent to NASA's mission.

Specialized services also include organizing and publishing research results, distributing specialized research announcements and feeds, providing information desk and personal search support, and enabling data exchange services.

For more information about the NASA STI Program, see the following:

- Access the NASA STI Program home page at http://www.sti.nasa.gov

NASA/ TM–20260001875

Modeling Study of Hatch Spacing's Effect on Grain Morphology in Repairing Damaged Metal Parts with Welding and Hatch Spacing's Potential Use in Lunar Exploration

Fredrick N. Michael
Marshall Space Flight Center, Huntsville, Alabama

Wei Li
The University of Texas at Dallas, Richardson, Texas

NASA Aeronautics and
Space Administration

Marshall Space Flight Center
Huntsville, Alabama

May 2026

Available from:

NASA STI Program / Mail Stop 050
NASA Langley Research Center
Hampton, VA 23681-2199

Table of Contents

Abstract

The welding process is a potential way of repairing a damaged metal component, especially cavity damage caused by a harsh environment like the lunar environment, which is characterized by large temperature differences and reduced gravity. The adjustment of welding parameter (e.g., hatch spacing) can improve production efficiency in the repair process. Seen from the microstructural level, hatch spacing sensitivity affects the metallic grain evolution and morphology in the welding process, which can further influence a repaired part's mechanical properties; however, the study of hatch spacing's effect on microstructure is challenging. Traditional experimental procedures are costly and time-consuming, and any change in hatch spacing value needs roll-back of experimental procedure. A modeling study can address the above challenges in experimental observation. In this research, a modeling approach based on the Kinetic Monte Carlo (KMC) Potts theory was used to simulate grain evolution and morphology with three hatch spacings. Through quantifying and analyzing the predicted grain morphologies, the effect of hatch spacing on microstructure in a welding-fabricated part was investigated. The predicted grain morphologies were validated with an EBSD image of welding microstructure, which has been published before. The primary grain morphologies were columnar grains with a small amount of fine equiaxed grains formed in the scanning path centerline. When increasing the hatch spacing, the columnar grains become larger and lengthier, while the effect of hatch spacing on the equiaxed grains is not obvious.

Keywords: Welding for repairing, hatch spacing, Kinetic Monte Carlo (KMC) Potts model, microstructure evolution

1.0 Introduction

The welding process is a potential technique that can repair metal components serving in an extreme environment [1−6]. Flexible welding paths and portable operations enable the welding process to be an effective manufacturing technique in repairing damaged metal parts with specific geometry and shapes used in various aircraft and systems (as shown in Fig.1). Lunar exploration needs various metal equipment, facility, and components. The harsh environmental conditions on the Moon surface could cause damage and failure of metal components that require repair operations with welding. The welding process applies a mobile laser beam to locally melt the wire addition following pre-designed scanning strategies. Steep temperature gradient is created in welding parts through the spatially and temporally moving laser heat source, which leads to a rapid cooling rate. Such high cooling rate yields heterogeneous microstructures involving elongated columnar grains and equiaxed grains. During the welding process, the printing parameters show significant impact on the grain morphology in the microstructure [7]. Hatch spacing is one important process parameter in the welding process parameter group; it is the distance between two adjacent laser scanning paths. Adjustment of hatch spacing can effectively control internal void in welding a part and improve production efficiency. Most importantly, different hatch spacings can affect the grain morphology in the microstructure. For example, smaller hatch spacing can close the adjacent scanning paths so more grains formed in the previous scanning path will be involved in the melting/solidification process in the subsequent scanning path. Investigating hatch spacing's effect on grain morphology is important since the mechanical properties of repaired part sensitively vary with the microstructure's inhomogeneity. The influence of hatch spacing on grain evolution and morphology has been studied with experimental approach and discussed previously [8−11]. However, traditional material characterizations with experimental methods are costly and time-consuming. If the hatch spacing parameter is not constant, the entire experimental material characterization procedures have to be repeated from specimen preparation, etching, observation, to data analysis. Most importantly, understanding microstructural evolution during rapid solidification provides insights into the optimization of the welding process and the linkage of processing and microstructure.

Figure 1. In-space welding used for repairing a damaged metal cavity.

In order to efficiently investigate hatch spacing's effect on grain morphologies formed in the welding process and link the welding process with microstructure evolution, a KMC Potts modeling approach was used in this work. Three increased hatch spacing values (1.5 mm, 1.75 mm, and 2 mm) were defined in three welding simulation cases. The simulated grain morphologies were then quantified and analyzed to study hatch spacing's effect.

2.0 Modeling Approach: Kinetic Monte Carlo Potts Model

The KMC Potts model was utilized as the modeling approach in this work. In a KMC Potts model, a microstructural grain is indicated using a group of lattice sites that are assigned with an integer index. All sites in a grain are defined with the same index value. The interfaces between the nearest neighboring sites with different indices are used to indicate grain boundaries [12−14]. The grain growth in welding or metal additive manufacturing process is determined by minimizing the grain boundary energy, i.e., calculated through the summation of the bond energy of neighboring lattice sites with different index values [7, 15, 16]. The calculation is performed using Eq. 1, where *N* is the total number of lattice sites; q_i and q_j are the index at the grain lattice sites *i* and *j*; and *L* is the number of neighbors of each grain lattice site. A factor of 0.5 is applied to eliminate double-counting in the summation [7, 16]. One energy unit is contributed by each pair of different neighboring sites to the total system energy. The simulation of grain growth begins with reassigning a lattice site's index to a different neighboring site randomly. This step causes a change in the overall system energy. The total energy of the system is recalculated with Eq. 1. Grain growth will happen if the index reassignment is accepted; otherwise, if the index reassignment is rejected, the grain growth will not happen. The probability of accepting the index reassignment is determined by the Metropolis function in Eq. 2 [7], where ΔE is the system energy change; k_B is Boltzmann's constant; and T_s is the local site temperature. The index reassignment is successful if the energy change is less than zero, which means there is a decrease in system energy and grain growth will happen. Then, if the energy change is positive, the probability of grain growth or grain boundary migration will follow the Boltzmann distribution.

$$E = \frac{1}{2}\sum_{i=1}^{N}\sum_{j=1}^{L}\left(1-\delta\left(q_i, q_j\right)\right) \tag{1}$$

$$P = \begin{cases} exp\left(\frac{-\Delta E}{k_B T_s}\right) & if\ \Delta E > 0 \\ 1 & if \Delta E \leq 0 \end{cases} \tag{2}$$

$$M = M_0\, exp\left(\frac{-Q}{RT(t,i)}\right) \tag{3}$$

$$P = \begin{cases} M * \exp\left(\frac{-\Delta E}{k_B T_s}\right) & if\ \Delta E > 0 \\ M & if \Delta E \leq 0 \end{cases} \tag{4}$$

In the laser welding process, the incident laser beam locally melts the metal substrate, forming a molten zone with intense thermal activity. Simultaneously, heat conduction from the molten zone into the surrounding solid material creates a heat-affected zone (HAZ) [17−19] characterized by steep temperature gradients and rapid thermal cycling. Grain evolution during welding is governed by the coupled effects of molten pool dynamics and solid-state microstructural transformations within the HAZ. As a result, both the mobility of the solid–liquid interface in the molten zone and the temperature-dependent grain boundary mobility in the HAZ play key roles in determining the final grain-level microstructure. In order to simulate this process, some adaptations were made to the above KMC-Potts model. A grain boundary mobility with the local temperature is defined in Eq. 3 [7], where constant Q is the activation energy for grain boundary motion; M_0 is the Arrhenius pre-factor; R is the gas constant; and $T(t,i)$ is the local temperature with time t and location i. Then the probability of accepting the index reassignment for grain evolvement in the welding process is updated in Eq. 4 [7, 15]. Figure 2 shows a mechanism of grain evolvement in the welding process simulated with the KMC Potts model. A 3D view of the grain evolution with the molten pool and solidification boundary are schematically illustrated. As the molten pool advances along the weld path, the material in the trailing region rapidly solidifies, and the steep temperature gradients drive accelerated grain growth. Within the KMC Potts framework, microstructural evolution is represented through Monte Carlo state transitions, where lattice sites probabilistically switch their grain indices to minimize local interfacial energy. These index reassignment events can occur in two ways: (1) adoption of indices from previously solidified neighboring grains, corresponding to grain growth driven by interface curvature and temperature-dependent mobility or (2) reassignment among lattice sites newly emerging from the molten pool, representing grain nucleation during solidification. Together, these processes capture the competitive growth and nucleation dynamics that shape the evolving weld microstructure.

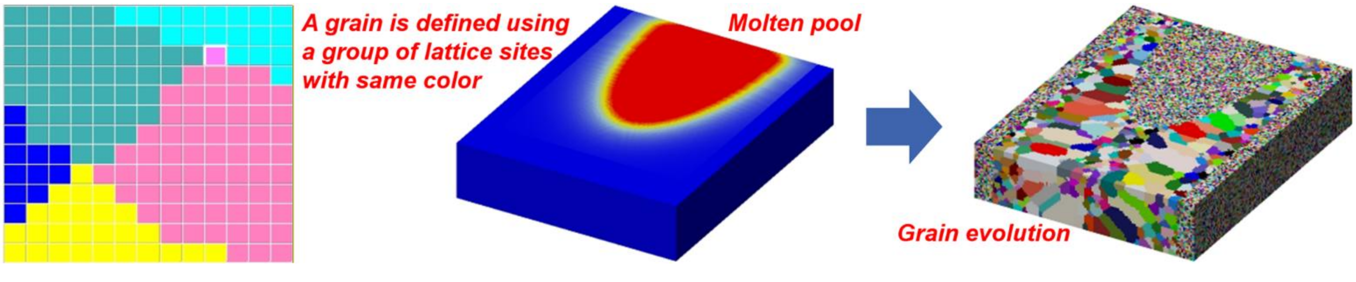

(a) (b) (c)

Figure 2. Grain and boundary in KMC Potts: (a) any single grain is defined with lattice sites with same color; (b) mobility function in the KMC Potts model; (c) simulated grain evolution.

The references [7, 15, 16, 20−21] introduced the details of how to simulate grain evolution with the KMC Potts model. To achieve high simulation efficiency and guarantee sufficient simulation accuracy, some assumptions were defined to neglect the unimportant details in the welding process according to the reference journal [18]. The welding process parameters and their definitions in the KMC model were referred from the journal [7]. These welding parameters include laser power (2 kW), spot size (4 mm), and transverse speed (600 mm/min). Three hatch spacing values are selected as 1.5 mm, 1.75 mm, and 2 mm. Figure 2 describes the simulation domain. Three SS304L specimens were repaired with the three hatch spacings.

3.0 Simulation Results and Analysis

3.1 Description of Predicted Grains

The top view (Fig. 3) was selected to observe the grain morphologies with three increased hatch spacings. Columnar grains were the primary microstructure formation, and small equiaxed grains formed near the scanning path's centerline. These morphologies are caused by the melted pool motion in welding repair or additive manufacturing. Materials input in the welding process are locally melted and then solidified with fast movement of a laser beam. The grain growth is driven by the high cooling rate and temperature gradient. Different hatch spacings result in varying melted pool moving history, which can cause different grain morphologies. Another finding is the relationship between grain morphology and hatch spacing. With increasing hatch spacing values, the size of columnar grains is increased. From the observation of simulated grain morphology, the columnar grains are larger and lengthier when the hatch spacing was 2 mm; when the hatch spacing was 1.5 mm, the columnar grains are shorter than the other two cases. Larger hatch spacing provides more space for columnar grain to coarsen, while smaller hatch spacing limits the grain growth. In addition, the equiaxed grain morphologies are not obviously affected by different hatch spacings.

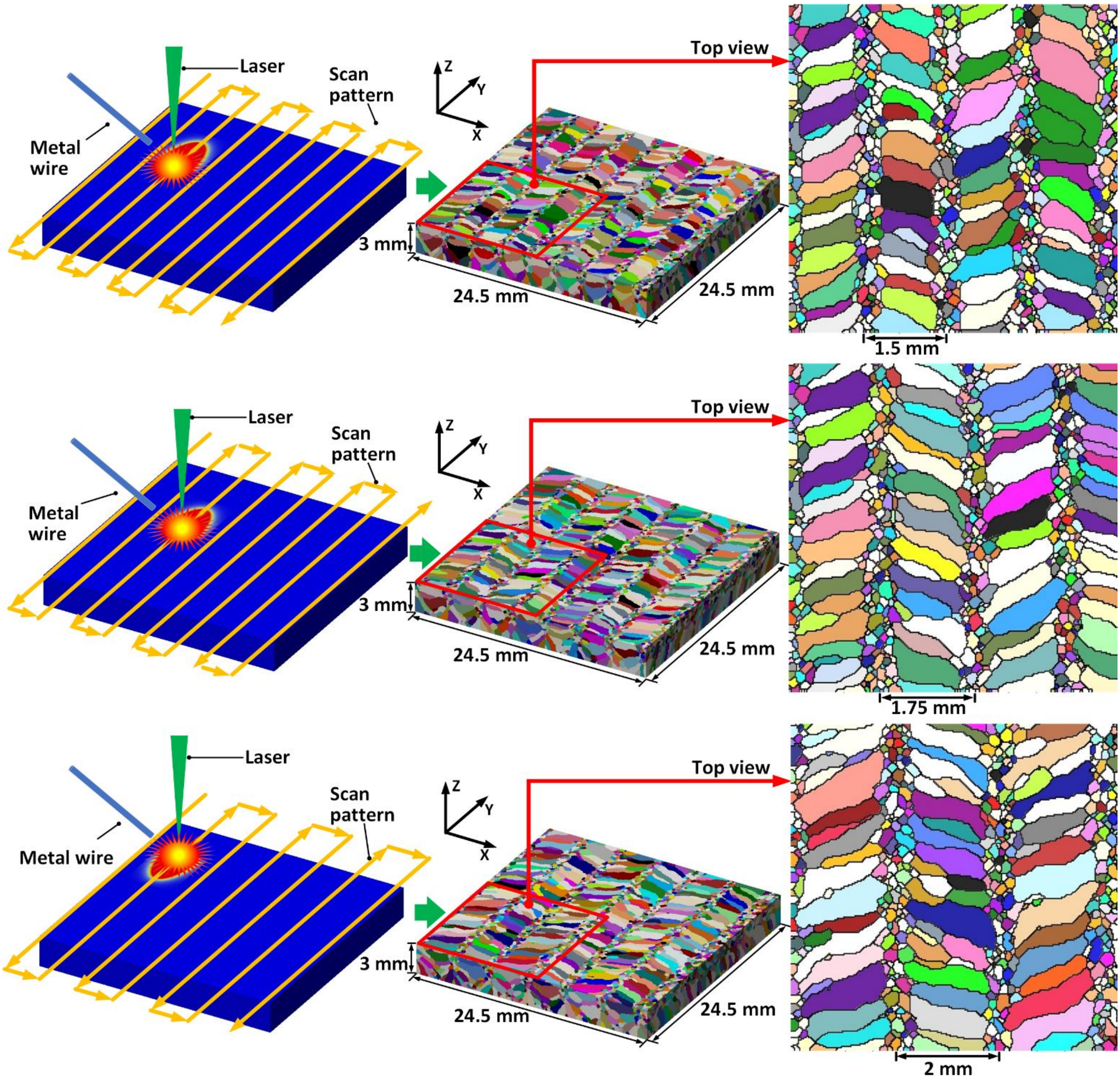

Figure 3. Simulated grain morphologies with three hatch spacings (1.5 mm, 1.75 mm, and 2 mm).

3.2 Quantifying the Simulated Grain Morphologies

It is necessary to quantify the distinctive grain morphology generated in welding repair. In this study, the Image J software was used to quantify the grain morphologies under different hatch spacings. Two quantification parameters were considered: (1) aspect ratio and (2) grain size. Illustrations of aspect ratio and grain size are shown in Figure 4. An ellipse is applied to best fit a grain. The aspect ratio of the grain is the ratio of the ellipse's minor axis and major axis [22]. The aspect ratio of the grain is a number ranging between zero and one. If aspect ratio is close to zero, this means the grain cross-section is nearly circular. If aspect ratio is close to one, the grain cross-section has a needle-like shape. Grain size is the dimension of the major axis of fit ellipse [20].

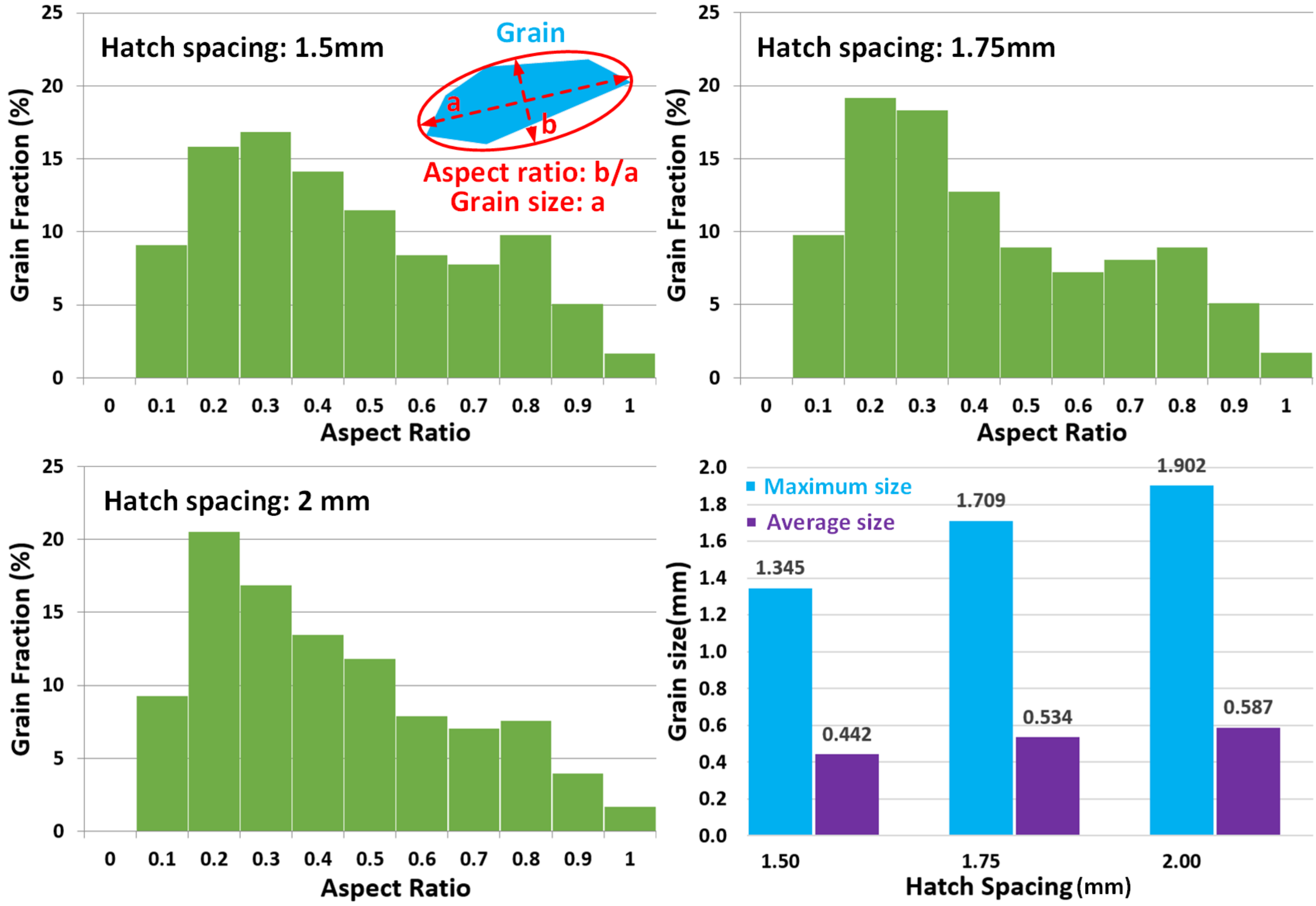

Figure 4. Grain aspect ratios and grain sizes under different hatch spacings.

Figure 4 shows the grain aspect ratio and grain size's histograms. Under different hatch spacings, the grain aspect ratio values were less than one. More than 50% of aspect ratio values were less than 0.6, which means a majority of grains have columnar morphologies. The first aspect ratio peak occurred near 0.2 and 0.3. The grains with this aspect ratio are shown as lengthy or elongated shape. Under the hatch spacing of 1.5 mm, the aspect ratio peak is approached to 0.3; and when the hatch spacing is increased to 2 mm, the aspect ratio peak is moved to 0.2. This means larger hatch spacing can generate much lengthier grains. The second grain aspect ratio peak occurred near 0.8. The grains with this aspect ratio are equiaxed grains. By observing Figure 3, it is apparent that some amount of equiaxed grains formed near the laser scanning path centerline. The second aspect of ratio peak at 0.8 can explain the formation of these equiaxed grains. In addition, different hatch spacings did not obviously affect the location of the second aspect ratio peak.

Besides the grain aspect ratio, another important indicator is grain size, which can quantitatively describe the effect of hatch spacing on microstructural morphology. Clearly both maximum value and average value of grain size increased under increasing hatch spacing. In the welding process, larger hatch spacing value easily provides more sufficient space for grain growth. The quantified grain size results in Figure 4 can explain the direct view of simulated grain morphologies in Figure 3.

3.3 Validation with Experimental EBSD Results

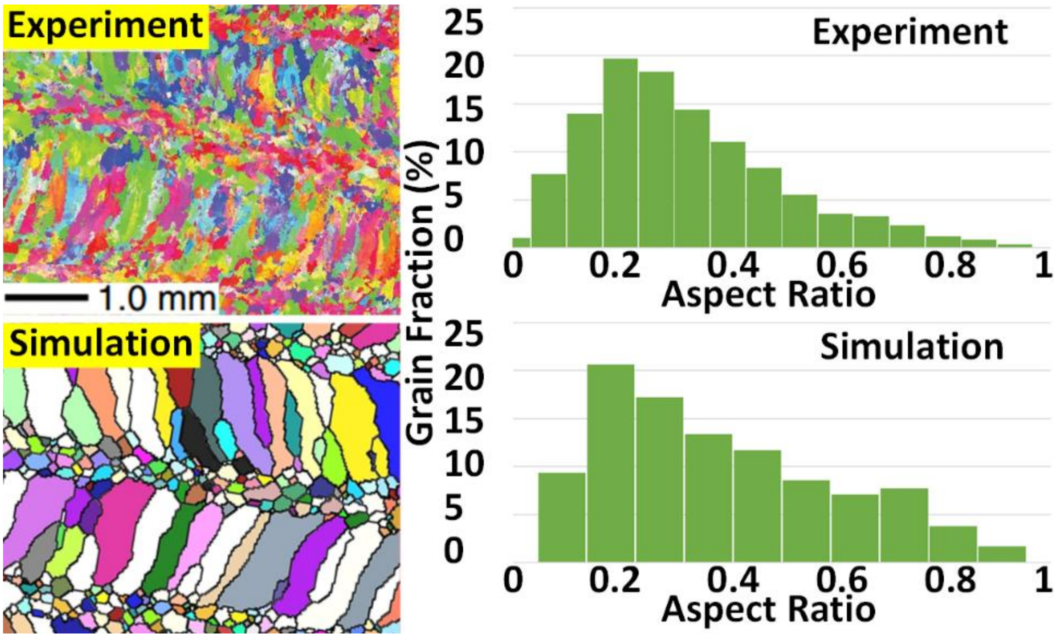

Figure 5. Grain aspect ratio comparison in experiment [7] and simulation results.

In order to validate the KMC Potts model, an EBSD image of a SS 304L welding specimen was referred from the journal [7] (Fig.5). The welding process parameters are the same in both the welding experiment and simulation cases. The hatch spacing in this case is 2 mm. The validation indicator is aspect ratio. The maximum grain fraction occurred at an aspect ratio of 0.2. The experimental EBSD image and the simulated grain morphology matched well. Furthermore, similar grain fraction trends can be observed in both the experimental EBSD and simulated grain morphology. The trends increase from zero to 0.2, and then gradually attenuate to zero.

4.0 Conclusion

The conclusions of this study are stated as follows. Columnar grain is the primary grain morphology formed in the welding process. A small amount of small equiaxed grains appeared near the laser scanning path centerline. These features are very close under different hatch spacings. With the increasing hatch spacing values, the size of columnar grains is increased, since larger hatch spacing provides more space for columnar grains to coarsen. For the equiaxed grains, different hatch spacings did not obviously affect the grain morphologies. Adjusting the hatch spacing changes the grain morphology, the fractions of the columnar grains, and fine equiaxed grains in the microstructure. Therefore, based on the current progress in modeling grain evolution in the welding process, the outlook of this study is focused on tailoring the grain-level microstructure by optimizing the hatch spacing.

References

[1] Li, W., X. Chen, L. Yan, J. Zhang, X. Zhang, F. Liou, "Additive manufacturing of a new Fe-Cr-Ni alloy with gradually changing compositions with elemental powder mixes and thermodynamic calculation," *International Journal of Advanced Manufacturing Technology*, 1–11, 2017.

[2] Li, W., L. Yan, X. Chen, J. Zhang, X. Zhang, F. Liou, "Directed energy depositing a new Fe-Cr-Ni alloy with gradually changing composition with elemental powder mixes and particle size effect in fabrication process," *Journal of Materials Processing Technology*, 255, 96–104, 2018.

[3] Li, W., S. Karnati, Y. Zhang, F. Liou, "Investigating and eliminating powder separation in pre-mixed powder supply for laser metal deposition process," *Journal of Materials Processing Technology*, 254, 294–301, 2018.

[4] Li, W., L. Yan, S. Karnati, F. Liou, J. Newkirk, K.M.B. Taminger, W.J. Seufzer, "Ti-Fe intermetallics analysis and control in joining titanium alloy and stainless steel by Laser Metal Deposition," *Journal of Materials Processing Technology*, 242, 39–48, 2017.

[5] Fujishima, M., Y. Oda, R. Ashida, K. Takezawa, M. Kondo, "Study on factors for pores and cladding shape in the deposition processes of Inconel 625 by the directed energy deposition (DED) method, CIRP," *Journal of Manufacturing Science and Technology*, 19, 200–204, 2017.

[6] Li, W., X. Zhang, F. Liou, "Modeling analysis of argon gas flow rate's effect on pre-mixed powder separation in laser metal deposition process and experimental validation," I*nternational Journal of Advanced Manufacturing Technology*, 1–11, 2018.

[7] Rodgers, T.M., J.D. Madison, V. Tikare, Simulation of metal additive manufacturing microstructures using kinetic Monte Carlo, *Computational Materials Science*, 135, 78–89, 2017.

[8] Liu, S., W. Yang, X. Shi, B. Li, S. Duan, H. Guo, J. Guo, "Influence of laser process parameters on the densification, microstructure, and mechanical properties of a selective laser melted AZ61 magnesium alloy, *Journal of Alloys and Compounds*, 808, 151–160, 2019.

[9] Wang, J., W.J. Wu, W. Jing, X. Tan, G.J. Bi, S.B. Tor, K.F. Leong, C.K. Chua, E. Liu, "Improvement of densification and microstructure of ASTM A131 EH36 steel samples additively manufactured via selective laser melting with varying laser scanning speed and hatch spacing," *Materials Science and Engineering: A 746*, 300–313, 2019.

[10] Kong, C.-J,, C.J. Tuck, I.A. Ashcroft, R.D. Wildman, R. Hague, "High density Ti6Al4V via SLM processing: microstructure and mechanical properties," *International Solid Freeform Fabrication Symposium*, 475–483, 2011.

[11] Nadammal, N., S. Cabeza, T. Mishurova, T. Thiede, A. Kromm, C. Seyfert, L. Farahbod, C. Haberland, J.A. Schneider, P.D. Portella, "Effect of hatch length on the development of microstructure,

texture and residual stresses in selective laser melted superalloy Inconel 718," *Materials & Design*, 134, 139–150, 2017.

[12] Holm, E.A., C.C. Battaile, "The computer simulation of microstructural evolution," *JOM*, 53(9), 20–23. 2001.

[13] White, R.J., "The development of grain-face porosity in irradiated oxide fuel," *Journal of nuclear materials*, 325(1), 61–77, 2004.

[14] J.E.R. Bishop, Theron Bishop, Kyle Johnson, Judith Alice Brown, "Simulating the mechanical response of synthetic AM microstructures generated with Kinetic Monte Carlo techniques.," 2016. https://www.osti.gov/biblio/1375297.

[15] Rodgers, T. M., J.D. Madison, V. Tikare, M.C. Maguire, "Predicting mesoscale microstructural evolution in electron beam welding," *JOM*, 68(5), 1419–1426, 2016.

[16] Rodgers, T.M., J.A. Mitchell, V. Tikare, "A Monte Carlo model for 3D grain evolution during welding, Modelling and Simulation in Materials Science and Engineering," 25(6), 064006. 2017.

[17] Wei, H., J. Elmer, T. DebRoy, "Three-dimensional modeling of grain structure evolution during welding of an aluminum alloy," *Acta Materialia*, 126, 413–425, 2017.

[18] Wei, H., J. Elmer, T. DebRoy, "Crystal growth during keyhole mode laser welding," *Acta Materialia*, 133, 10–20 2017.

[19] Wei, H., G. Knapp, T. Mukherjee, T. DebRoy, "Three-dimensional grain growth during multi-layer printing of a nickel-based alloy Inconel 718," *Additive Manufacturing*, 25, 448–459, 2019.

[20] Li, W., M. Soshi, "Modeling analysis of the effect of laser transverse speed on grain morphology during directed energy deposition process," *International Journal of Advanced Manufacturing Technology,* 3279–3291, 2019.

[21] Li, W., M. Soshi, "Modeling analysis of grain morphologies in Directed energy deposition (DED) coating with different laser scanning patterns," *Materials Letters*, 251, 8–12, 2019.

[22] Ferreira, T., W. Rasband, *ImageJ user guide*, IJ, 2015.